**Anatolii D. Pomogailo**, **Aleksander S. Rozenberg**, **Gulzhian I. Dzhardimalieva**
Institute of Problems of Chemical Physics, Russian Academy of Sciences Chernogolovka, Russia
**Marcin Leonowicz**
Faculty of Materials Science and Engineering, Warsaw University of Technology, Poland

# POLYMER NANOCOMPOSITES ON THE BASE OF METAL CARBOXYLATES

ABSTRACT

The thermal transformation of unsaturated metal carboxylates (metal acrylates and maleates) are the complex process including dehydration, solid phase polymerization, and decarboxylation of metalcarboxylate groups of the polymer formed which proceed sequentially at varied temperature ranges. The thermolysis resulted in the synthesis of metal nanoparticles with narrow size distribution (the mean particle diameter of 5-10 nm) in the polymer matrix formed *in situ*.

## INTRODUCTION

Metal-polymer composites possessing specific physicochemical and mechanical properties are widely used as optical and magnetic materials, catalysts of various reactions, drugs in medicine and coatings. Numerous procedures for the preparation of nanocomposite materials are available: evaporation of elemental metal with its deposition on polymeric matrices, plasma--induced polymerization, vacuum evaporation of metals, thermal decompositions of precursors in the presence of polymers and reduction of metal ions, etc. [1]. Thermal transformations of metal--containing monomers have attracted considerable recent attention because they can result in the formation of metal nanoparticles stabilized in the polymer matrix [2]. The main advantage of synthesis of composites by thermal transformation of metal-containing precursors is the possibility of formation of nanocomposites at the relatively high concentration of metal phase using relatively simple technology, and the control of processes and properties of materials obtained. The present work has been aimed to study the kinetic peculiarities of thermal transformation of transition metal acrylates and maleates as well as properties metal-polymer nanocomposites formed.

## EXPERIMENTAL

Metal carboxylates were synthesized according to procedures described earlier [3, 4]. The cocrystallite iron acrylate·nickel acrylate ($Fe_2NiAcr$) was prepared by coprecipitation of salts $FeAcr_3$ and $NiAcr_2$ from alcoholic solution. The Fe/Ni ratio is 2:1. For $Fe_2NiAcr$: found (%): Fe, 16.8; Ni, 8.9. $[Fe_3O(CH_2CHCOO)_6OH]\cdot[Ni(CH_2CHCOO)_2]_{1.5}\ 3H_2O$. Calcd (%): Fe, 17.08; Ni, 9.12. The Fe/Ni ratio is 1.98.

Thermal transformations of metal carboxylates were studied in a self-generated atmosphere (SGA) and under a static isothermic condition. The kinetics of gas evolution were recorded using

a membrane zero-manometer. The mass loss of the sample (Δm, wt. %) and the amounts of gaseous products at ~20ºC and those condensing at 77 K were determined at the end of the experiments. The volume of the heated tube did not exceed 0.05 *V*. The ratio $m_0/V = (0.60–3.85)\cdot10^{-3}$ g cm$^{-3}$, where $m_0$ is the initial weight of the sample. The specific surface ($S_{sp}$) of the initial samples and the solid-phase products of their thermal transformation were determined by the low temperature nitrogen adsorption method.

Elemental analysis was performed by the atomic absorption method on a Saturn instrument and by the combustion method. The magnetic susceptibility was measured by the Faraday method at 77 and 292 K. The magnetic moment was calculated by the formula $\mu_{eff} = 2.84\sqrt{\chi_{at}T}$, where $\chi_{at}$ is the magnetic susceptibility based on a 1 g-at. metal standard. Magnetic measurements were carried out on a PAR-155 vibration magnetometer. Optical mircoscopic analysis was performed in the transmitted light mode on a MBI-15 Leitz Metalloplan instrument. An IEM-1200Ex instrument (accelerating voltage 120 kV) was used for electron microscopic studies. Samples were prepared as a suspension of a powdered substance in ethanol, which was then deposited on a carbon film substrate. Mass spectral analysis was performed on a MS 3702 quadruple mass spectrometer. IR spectra were recorded on a Perkin-Elmer 325 and Specord IR 75 spectrophotometers, and the samples were prepared as pellets with KBr.

## RESULTS AND DISCUSSION

The carboxylates studied include transition metal acrylates, $(CH_2 = CHCOO)_2Cu$ ($CuAcr_2$), $(CH_2 = CHCOO)_2Co\cdot2H_2O$ ($CoAcr_2$), $(CH_2 = CHCOO)_2Ni\cdot2H_2O$ ($NiAcr_2$), $[Fe_3O(OH)(CH_2 = = CHCOO)_6\cdot 3H_2O]$ ($FeAcr_3$), cocrystallite $NiAcr_2$ and $FeAcr_3$ with Fe:Ni = 2:1 as well as cobalt, $Co[OOCCH = CHCOO]\cdot2H_2O$ CoMal), and iron, $Fe_3O(OH)[OOCCH = CHCOOH]_6\cdot3H_2O$ (FeMal) maleates. Thermolysis of monomers under study is accompanied by gas evolution and mass loss due to dehydration and subsequent thermal transformation of the dehydrated specimens. The processes proceed sequentially at varied temperature ranges.

*Dehydration*. According to thermal analysis, the temperature ranges of dehydration of the monomers have been found to be 353–487 K ($FeAcr_3$), 413–453 K ($CoAcr_2$), 373–473 K ($NiAcr_2$), 393–433 K (CoMal), and 373–433 K (FeMal). The dehydration resulted in a disappearance of absorption bands in the IR spectra attributed to the modes of crystal water [5]: ν(O–H) 3000– –3600 cm$^{-1}$, $\rho_\omega$(O–H) + ν(Co–$OH_2$) 880 cm$^{-1}$. This was accompanied by decreases in the intensity of modes associated with δ(O–H) + ν(C = C) 1655 cm$^{-1}$, $\rho_\omega(CH_2)$ + δ(Co–$OH_2$) 690 cm$^{-1}$, δ($CH_2$) + + δ( Co–$OH_2$) 595 cm$^{-1}$.

*Polymerization*. Increasing temperature up to $<T_{term}>$ = 473–573 K results in solid phase polymerization of the dehydrated monomer. At this temperature range, under conditions of thermal analysis and self-generated atmosphere (SGA), the thermal transformations of the monomers are accompanied by slight mass loss (<< 10 wt. %) and small gas evolution. According to the data of TA [6-9], representative temperatures ($T_{polym}$) at which polymerization proceeds as follows: ~543 K ($CoAcr_2$), ~563 K ($NiAcr_2$), ~510 K ($CuAcr_2$), ~518 K ($FeAcr_3$), 488–518 K (CoMal), ~518 K (FeMal). During polymerization, changes in absorption IR-spectrum were observed. These changes are associated with the decrease in the intensity of the absorption band of the stretching vibrations of the C = C bond and contraction in the vibration frequencies resulted in appearance of a web absorption band in the region of 1540-1560 cm$^{-1}$. Thermolysis of FeMal mass loss by the sample amounts to 31.25 and 8.75 wt. %, respectively at maximum DTA temperatures of 433 and 518 K respectively. The first thermal effect (strong effect) is related to both the dehydration process (5.2% for the loss of three water molecules) and, most likely, partial

desolvation of three molecules of maleic acid (36.8% is the calculation for complete desolvation). The weak endoeffect accompanying the mass loss in the second region is most likely caused by polymerization of the desolvated monomer. As a rule, in these regions $\Delta m$ is ~40%, which is close to the loss of three water molecules and three molecules of maleic acid (calculated value of 42%).

*Kinetics of Decarboxylation*. At $T_{term} > 523$ K (for $CuAcr_2$ $T_{term} > 453$ K) intensive gas evolution of thermal polymerized samples was observed. Kinetic details of this process were studied in the isothermal SGA-regime for $CuAcr_2$ ($<T_{term}> = 363–513$ K), $CoAcr_2$ (623–663 K), $NiAcr_2$ (573–633 K), $FeAcr_3$ (473–643 K), FeCoAcr (613–633 K), $Fe_2CoAcr$ (613–633 K), $Fe_2NiAcr$ (603–643 K), CoMal (613–643 K), FeMal (573–643 K). The rate of gas evolution, $W = d\eta/dt$, decreases monotonically with the extent of conversion, $\eta = \Delta\alpha_{\Sigma,\,t}/\Delta\alpha_{\Sigma,\,f}$, where $\Delta\alpha_{\Sigma,\,t} = \alpha_{\Sigma,\,t} - \alpha_{\Sigma,\,0}$, $\Delta\alpha_{\Sigma,\,f} = \alpha_{\Sigma,\,f} - \alpha_{\Sigma,\,0}$, $\alpha_{\Sigma,\,f}$, $\alpha_{\Sigma,\,t}$ and $\alpha_{\Sigma,\,0}$ are the final, current and initial number of moles of gaseous products released per mole of the starting substance at $T_{room}$, respectively. The kinetics of gas evolution $\eta(\tau)$ in a general way (up to $\eta \le 0.95$) is satisfactorily approximated by the equation for two parallel reactions:

$$\eta(\tau) = \eta_{1f}[1 - \exp(-k_1\tau)] + (1 - \eta_{1f})[1 - \exp(-k_2\tau)], \quad (1)$$

where $\tau = t - t_0$ ($t_0$ is the time of heating); $\eta_{1f} = \eta(\tau)\,|\,k_{2t\to 0},\, k_{1t\to\infty}$, $k_1$, $k_2$ are the effective rate constants. The parameters of $k_1$, $k_2$, $\eta_{1f}$, and $\Delta\alpha_{\Sigma,\,f}$ depend on $T_{term}$ in the following manner:

$$\eta_{1f},\, \Delta\alpha_{\Sigma,\,f} = A\exp[-E_{a,eff}/(RT_{term})],\quad k_{eff} = k_{0,eff}\exp[-E_{a,eff}/(RT_{term})],$$

where A, $k_{0,eff}$ is pre-exponential multiplier [$sec^{-1}$], $E_{a,eff}$ is the activation energy [kJ/mol].

The initial rate of gas evolution $W_{\tau=0} = W_0$ will be

$$W_0 = \eta_{1f}k_1 + (1 - \eta_{1f})k_2 \quad (2)$$

The kinetics of gas evolution on the thermolysis of $NiAcr_2$, $Fe_2NiAcr$, FeMal are described by equations (1) and (2).

At $k_2 \approx 0$, $\eta_{1f} \to 1$

$$\eta(\tau) \approx 1 - \exp(-k_1\tau),\ W_0 \approx k_1. \quad (3)$$

These kinetic equations were used for thermolysis of $CoAcr_2$, CoMal.

When $\tau << 1/k_2$, $k_1 >> k_2$,

$$\eta(\tau) \approx \eta_{1f}[1 - \exp(-k_1\tau)] + (1 - \eta_{1f})k_2\tau,\ W_0 \approx \eta_{1f}k_1 \quad (4)$$

Equation (4) describes the kinetics of gas evolution of $CuAcr_2$. The change of $m_0/V$ does not affect the rate of thermolysis. Two gas evolution regions were observed in the decomposition of $FeAcr_3$: a low-temperature region ($<T_{term}> = 473–573$ K) and high-temperature region ($<T_{term}> = 603–643$ K) (Fig. 1). Here the rate of gas evolution is well approximated by equation (3) but with different values of $k$ and $\Delta\alpha_{\Sigma,\,f}$ (for instance, $k_1 = 4.2\cdot10^{21}\exp[-(59000\pm2500)/(RT)]\ c^{-1}$ and $k_2 = 1.3\cdot10^{6}\exp[-(30500\pm2000)/(RT)]\ c^{-1}$, respectively for low- and high temperature regions). The difference in kinetic parameters in the low- and high temperature regions for thermolysis of $FeAcr_3$ are governed by the presence of two parallel processes of gas evolution. The effective activation energy of gas evolution ($E_{a,eff}$) for $CuAcr_2$ is 202.7 kJ/mol, and for

$NiAcr_2$ is 246,6 kJ/mol. These are in agreement with the calculated $E_{a,eff}$ values of thermolysis in the TA-regime [8]: 211.1 and 244.1 kJ/mol. At the same time, the value of $E_{a,eff}$ (238.3 kJ/mol) for $CoAcr_2$ in the SGA-regime is higher than that of the thermolysis in the TA-regime ($E_{a,eff}$ = 206.1 kJ/mol).

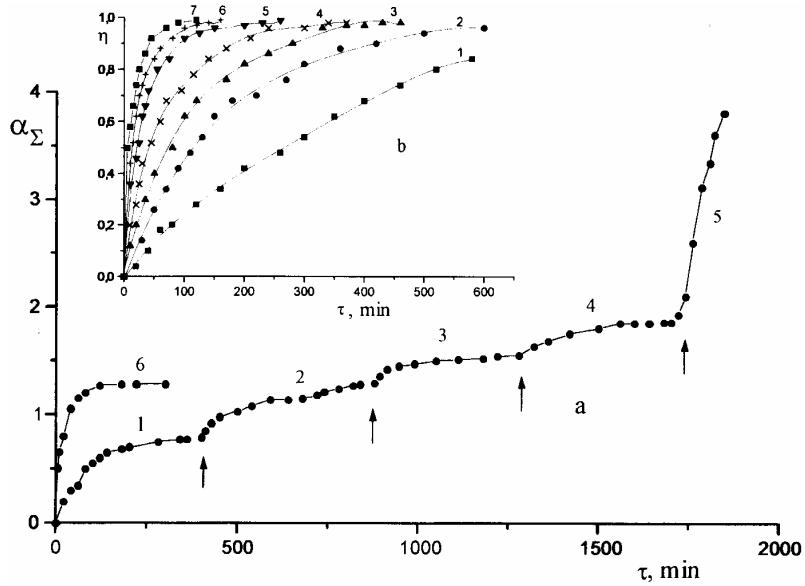


**Fig. 1.** (a) The kinetics of gas evolution from $FeAcr_3$ at $T_{exp}$ (°C): 1, 215; 2, 250; 3, 275; 4, 300; 5, 350; 6, 240. The moment of $T_{exp}$ increasing is shown by pointer. (b) Dependence η(T) on $T_{exp}$ (°C): 1, 200; 2, 205; 3, 210; 4, 215; 5, 220; 6, 230, 7, 240 ($m_o/v = 6.7\times10^{-3}$ g cm$^3$ where $m_o$ is start mass of sample)

*The products of thermal transformation*. The gaseous and condensed products. $CO_2$ is the main gaseous product of thermal transformation of acrylates, their cocrystallates.and maleates. This is confirmed by IR-spectroscopic (IR) and mass-spectroscopic (MS) studies. CO (IR, MS), H2 (MS) are evolved to a substantially smaller amount. Vapors of H2O condensed at Troom (IR, MS). $CH_2$ = CHC(O)OH (IR, MS), HOC(O)CH = CHC(O)OH (IR, MS) ligands were formed as products of pyrolysis of the corresponding complexes. $H_2O$ and $CH_2$ = CHC(O)OH or HOC(O)CH = CHC(O)OH evolution occurs at the first stage of transformation and is associated with dehydration and solid phase polymerization which are responsible for major gas evolution. This is confirmed by a comparison of the amounts of evolved gaseous products with mass loss by the samples. Along with the indicated gaseous products, $CH_4$ (IR, MS) was observed in the case of both $CoAcr_2$ (the traces) and $NiAcr_2$ (commensurable with $CO_2$ quantities). The products of thermal transformation of $CuAcr_2$ include also $C_2H_4$ of measurable quantities ((IR, MS). Mass loss by the sample at the end of gas evolution increases uniformly with $T_{term}$ but does not reach the values expected for metal carboxylate decay to a metal or its oxide.

*The topography of solid phase products*. The change in the topography of the solid phase in the course of conversion was monitored by optical microscopy (OM). The powders of metal carboxylates were characterized by high and similar dispersity (Table 1). The average size of the particles ($L_{S,av}$), calculated from $S_{0,sp}$, is 0.01–0.05 μm (without taking account of the coefficient of the form). This is substantially less than $L_{OM,\ av}$. Such differences between the $L$ values reveal high porosity of the starting samples, i.e., a block structure with diffusionaly transparent interblock boundaries. During thermolysis the sample specific surface $S_{sp,f}$ was found to increase

in the case of $CuAcr_2$, $CoAcr_2$, and $NiAcr_2$. Most of the changes occur at the earlier stage of conversion, and at the end $S_{sp,f}$ exceeds $S_{sp,0}$ by 2 to 3 times (Table 1).

***Table 1.*** *Dispersity of starting metal carboxylate samples and the thermolysis products*

| Sample | $S_{0,sp}$, $m^2/g$ | $S_{f,sp}$, $m^2/g$ | $L_{OM,av}$, μm |
|---|---|---|---|
| $CuAcr_2$ | 14,7 | 48,0 (463 K) – 53,8(473 K) – 43,8(503 K) | 5–50 |
| $CoAcr_2$ | 20,2 | 24,1 (623 K) – 42,1(663 K) | 100–150 |
| $FeAcr_3$ | 15,0 | 15,0 | 1–5 |
| $NiAcr_2$ | 16,0 | 55,0 – 60,5 | 60–100 |
| $Fe_2NiAcr$ | 8,5 | 13,5 | 100–200 |
| CoMal | 30,0 | 30,0 | 5–70 |
| FeMal | 24,0 | 26,0 | 30–50 |

In the case of $CuAcr_2$ the behavior of $S_{sp,f}$ ($T_{term}$) is unusual. Initially $S_{sp,f}$ increases with $T_{temp}$ up to 493 K, then it decreases. A decrease of $S_{sp,f}$ at $T_{term} > 493$ K is apparently governed by caking. However, in the thermal transformation of $FeAcr_3$, $Fe_2NiAcr$, CoMal and FeMal, the values of $S_{sp,f}$ do not change substantially.

Analysis of the data of specific surface and topography of the solid phase both during and at the end of thermolysis leads to supposition that metal carboxylates studied have the following common properties. At a low degree of gas evolution (during heating the sample) a loss of the particle transparency was observed. The surface of the particles becomes rough due to the desolvation processes, in particular, dehydration. In the case of $CoAcr_2$, $NiAcr_2$, and $CuAcr_2$, the dispersion proceeds during the transformation process, and the sizes of the formed particles are within $1 \div 10$ μm ($S_{sp,f}$ increases). For $FeAcr_3$, $Fe_2NiAcr$, CoMal and FeMal, no change in the dimension of particles and $S_{sp,f}$ was observed at the end of gas evolution. During gas evolution (at mass loss of 15-30%) the initial particles of $FeAcr_3$ are enlarged because of the formation of agglomerates which consist of porous, fragile glass-like plates with average sizes between 20 and 100 μm. During transformation, the sample transparency diminishes to become opaque by the end of the process that indicates the volume homogeneous process. The portion of these particles constitutes 40-60%. This fact indicates that the reactivities of particles are different. Together with the general loss of the particle transparency, the transformation process was observed in the macrodefects region as the formation of small opaque zones. At the late stage of thermolysis, small opaque particles ($< 1$ μm) are formed. In some cases ($FeAcr_3$, $NiAcr_2$) fractal-like structures as chain of agglomerates with average length of 50-70 μm were observed. They consist of 5-7 agglomerates of small particles.

Electron microscopy (EM) study of the products of metal carboxylates transformations is shown for $FeAcr_3$, CoMal, $Fe_2NiAcr$ to have similar morphology. It is characterized by practically spherical electron-dense clusters having a narrow size distribution and alloted in a low electron-dense matrix. The clusters are present both individually and as agglomerates from 3-10 particles. The nanosized particles are uniformly distributed in the matrix at an average distance of 8-10 nm. For CoMal along with nanosized spherical clusters relative large aggregates as cubic crystals of 10-20 nm size were observed (Fig. 2). The yield products of thermolysis, with the exception of $NiAcr_2$, were shown to be amorphous by x-ray. By the x-ray diffraction data, the product of $NiAcr_2$ thermolysis is a mixture of three phases (Ni-NiO-$Ni_3C$). The ratio of Ni

in the phases is Ni:NiO:$Ni_3C$ ≈ 0.51:0.81:1.0. By electron diffraction studies using EM, $Fe_3O_4$ and CoO were shown to be the main products of the $FeAcr_3$, FeMal, $CoAcr_2$, and CoMal thermolysis, respectively. *Magnetic properties of the $MAcr_n$ products of thermolysis*. With the exception of $CuAcr_2$ the products of thermal transformation of the metal carboxylates examined are ferromagnetic. Some magnetic properties of $Macr_n$ and their products of thermolysis are shown in Table 2. According to electron diffraction and x-ray analysis, $Fe_3O_4$ is the main product of $FeAcr_3$ thermolysis. However, the specific magnetization of $FeAcr_3$ thermolysis products ($\sigma_s$) is lower than that which could have been expected if all the Fe atoms in the decay products were present as $Fe_3O_4$ ferrite. Apparently the Fe atoms that do not contribute to the magnetization (~45 at. %) are present as an amorphous phase in the sample. An analogous picture is observed in the solid products of $NiAcr_2$ transformation.

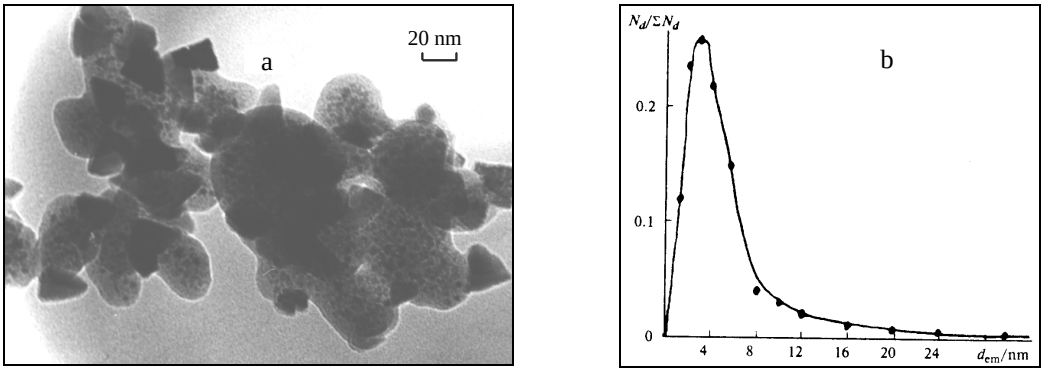


**Fig. 2.** (a) Electron microfraph of particles of the product of t hermolysis of CoMal ($T_{exp}$ = 350 °C, t = 9 h) (b) Distribution of electrondense particles in the product of thermolysis of CoMal; $N_d$ is the number of particles with the size $d$ ($\Sigma N_d$ = 390)

***Table 2.*** *The magnetic properties of some $MAcr_n$ and their thermolysis products*

| $MAcr_n$ | $\chi_\sigma \cdot 10^5$($cm^3$/g) found/calcd | | $\sigma_S$ (Gs·$cm^3$/g) | | $H_C$ (Oe) | | $j_r$ | |
|---|---|---|---|---|---|---|---|---|
| | 292 K | 77 K | 292 K | 77 K | 292 K | 77 K | 292 K | 77 K |
| $FeAcr_3$ | 1.75/5,50 | 3,22/21,0 | 0,152 | 0,306 | – | – | – | – |
| Product of $FeAcr_3$ | 26,1 | 26,1 | 33,45 | 35,94 | 22,0 | 233,0 | 0,051 | 0,25 |
| $NiAcr_2$ | 2,55/2,83 | 2,55/2,83 | – | 0,209 | – | – | – | – |
| Product of $NiAcr_2$ | 16,7 | 12,3 | 14,36 | 14,95 | 8,95 | 53,6 | 0,02 | 0,133 |
| $CoAcr_2$ | 4,83/2,93 | 15,1/11,15 | 0,442 | 1,41 | – | – | – | – |
| FeCoAcr | 2,73/3,17 | 6,50/8,63 | 0,258 | 0,742 | – | – | – | – |
| Product of FeCoAcr | 41,2 | 31,1 | 26,16 | 13,91 | 625,0 | 625,0 | 0,31 | 0,42 |

$\chi_\sigma$ is the magnetic susceptibility; $\sigma_s$ is the specific magnetization; $H_C$ is the coercive force; $j_r$ is the coefficient of rectangularity.

***Table 3.*** *The change of magnetic properties (in the magnetic field of ±10 kOe) during thermolysis of $NiAcr_2$ ($T_{term}$ = 643 K)*

| Δm (%, wt.) | $\sigma_S$ (Gs·cm$^3$/g) | | $\sigma_F$ (Gs·cm$^3$/g) | | $\chi_\sigma \cdot 10^5$(cm$^3$/g) | | $\eta_F = \sigma_F/\sigma_S$ | |
|---|---|---|---|---|---|---|---|---|
| | 300 K | 77 K | 300 K | 77 K | 300 K | 77 K | 300 K | 77 K |
| 0 | 0,209 | – | 0 | – | 2,55 | – | 0 | – |
| 19,1 | 0,235 | 0,675 | 0,024 | 0,041 | 2,19 | 6,7 | $4{,}4\cdot10^{-4}$ | $7{,}5\cdot10^{-4}$ |
| 27,1 | 0,323 | 1,447 | 0,084 | 0,155 | 2,53 | 11,8 | $1{,}5\cdot10^{-3}$ | $2{,}8\cdot10^{-3}$ |
| 35,4 | – | 2,177 | – | 0,24 | – | 9,9 | – | $2{,}3\cdot10^{-2}$ |
| 46,0 | 0,93 | 2,184 | 0,624 | 0,949 | 3,24 | 11,6 | $1{,}1\cdot10^{-1}$ | $1{,}7\cdot10^{-1}$ |
| 51,2 | 14,36 | 14,95 | 12,8 | 13,78 | 16,7 | 12,3 | $2{,}35\cdot10^{-1}$ | $2{,}5\cdot10^{-1}$ |

$\sigma_F$ is the specific susceptibility extrapolated to zero magnetic field.

The specific magnetization observed for the product of $NiAcr_2$ thermolysis (Table 3) is lower (only ~25 at. %) than the theoretical value of $\sigma_s$ in the case of Ni-phase ferromagnetism of samples ($\sigma_s$(Ni) = 54,5 Gs·cm$^3$/g). It was of interest to observe the evolution of magnetic properties during thermal transformation. Apparently this is associated with a drastic increase of the rate of ferromagnetic phase formation at the end of transformation. However, the parts by weight of the ferromagnetic phase of metal Ni in the sample ($\eta_F = \sigma_F/\sigma_s$(Ni), where $\sigma_s$(Ni) = 54.5 Gs·cm$^3$/g) amounts only to $\eta_F \approx 0.23$–$0.25$ at the end of conversion, i.e., the ferromagnetic phase contains 1/4 part of nickel atoms.

*Possible pathways of thermolysis.* It is anticipated that the structural units are principally preserved during dehydration of the initial carboxylates and their cocrystallites. At the same time the bidentate function of carboxyl groups becomes tridentate for some groups, which fulfill both a role of ligand and absent water molecules as is known for many desolvated and dehydrated carboxylates [10]. The increase in carboxyl group dentate degree results in a distortion in the oxygen environment of the metal. This leads to a change in the strength of the M-O and the C-O bonds. One can assume that with the increase in the level of heat vibrations in the lattice of the monomer a rupture of the weakest M-O bonds is most probable. As a result, mono- ($CH_2$=CHC(O)O$^\bullet$) and biradicals ($^\bullet$OC(O)CH=CHC(O)O$^\bullet$) are formed for acrylates and maleates, respectively. The formed radicals react with the metal-containing acrylate (maleate) fragments to give the corresponding acids and the H-depletion radical R$^\bullet$ of acrylic (maleic) groups:

Initiation

$$R^{\#}\text{=CHC(O)O}^\bullet + RH \rightarrow R^{\#}\text{=CHC(O)OH} + R^I,$$

where $R^{\#}$=$CH_2$, RH=[$CH_2$CHC(O)O]$M^{n+}{}_{1/n}$, $R^I$=[$^\bullet$CHCHC(O)O]$M^{n+}{}_{1/n}$ (in the case ofacrylates); $R^{\#}$=$^\bullet$OC(O)CHCHC(O)O$^\bullet$, RH=[CH(O)O]$_2M^{n+}{}_{2/n}$, $R^I$=[$^\bullet$CC(O)O]$_2M^{n+}{}_{1/n}$ (in the case of maleates).

The $R^I$ formed initiates the polymerization to produce linear or net polymers.

Polymerization

$$R^I + s[CH_2\text{=CHCOO}]M^{n+}{}_{1/n} \rightarrow R^I\text{–}[\text{–}CH_2\text{–}CH_{COOM1/n}\text{–}]_s\text{–}\ R^I$$

$$R^I + s[OOCCH\text{=}CHOO]M^{n+}{}_{2/n} \rightarrow R^I\text{–}[\text{–}_{M1/nOOC}CH\text{–}CH_{COOM1/n}\text{–}]_s\text{–}\ R^I$$

With thermal treatment, metal-containing fragments of produced polymers decompose to metal (or its oxide) with the evolution of $CO_2$.

Decarboxylation

$$R^I\text{–}[\text{–}CH_2\text{–}CH_{COOM1/n}\text{–}]_s\text{–}\ R^I \longrightarrow CH_2\text{=}CH\text{–}CH\text{=}CH\text{–}[\text{–}CH_2\text{–}CH\text{=}CH\text{–}CH_2\text{–}]_{s/2}\text{–}CH\text{=}$$
$$\text{=}CH\text{–}CH\text{=}CH_2 + 2(s\text{+}1)CO_2 + (s\text{+}2)M,$$

$$R^I\text{–}[\text{–}_{M1/n}OOC CH\text{–}CH_{COOM1/n}\text{–}]_s\text{–}\ R^I \rightarrow CH\equiv C\text{–}[\text{–}CH\text{–}CH\text{–}]_s\text{–}C\equiv CH + 2(s\text{+}2)CO_2 + (s\text{+}2)M.$$

The polymers produced in the decarboxylation reaction can be thermal polymerized to form the net structure with conjugated multiple bonds.

Thus, in a general way, the composition of solid phase products of thermolysis can be present as the C-H-O-fragment fractions:

$$MO_z(CH_2CHCOO)_{p-x}(CHCHCOO)_{q-y}(CH_2CH)_x(CHCH)_n, \quad \text{(for acrylates)}$$
$$MO_z(\text{=}CHCOO)_{2p-x}(\text{=}CCOO)_{2q-y}(\text{=}CH\text{–})_x(\equiv C\text{–})_n, \quad \text{(for maleates)}$$

where $x = y = z = 0$ ($z \neq 0$ in the case of $FeAcr_3$, FeMal), $p$ and $q$ is the amount of intra-chain and H-depletion terminal groups ($p + q = 1$), respectively. Metal oxides can be formed in the oxidation reactions:

$$M + \lambda_1 CO_2 = MO_z + (\lambda_1 - z)CO_2 + zCO,$$
$$M + \lambda_2 H_2O = MO_z + (\lambda_2 - z)H_2O + zH_2.$$

## SUMMARY AND CONCLUSION

The thermal transformation of unsaturated metal carboxylates consists of three subsequent macrostages:

1) dehydration of crystal hydrate monomers ($T_{term} < 423$ K) with simultaneous rebuilding of the ligand environment accompanied by the elimination of the part of the carboxylate ligands as acrylic or maleic acids;
2) solid phase polymerization and copolymerization of rebuilding dehydrated monomer ($T_{term} \approx 453$–$493$ K);
3) decarboxylation of (co)polymers formed at high temperatures ($T_{term} > 473$ K). In this stage the main gas evolution and mass loss by the sample were observed.

The thermolysis resulted in the synthesis of metal nanoparticles with narrow size distribution (the mean particle diameter of 5-10 nm) in the polymer matrix formed *in situ*. The features of thermal conversions in metal carboxylates make it possible to prepare polymer-immobilized nanoparticles of metals and metal oxides of desirable particle-size distribution

## REFERENCES

1. Pomogailo A. D., Rozenberg A. S., Uflyand I. E.: *Nanoscale metal particles in polymers.* Khimiya, Moscow, Russia, 2001.
2. Rozenberg A. S., Dzhardimalieva G. I., Pomogailo A. D.: *Polymer Composites of Nano-sized Particles Isolated in Matrix.* Polym. Adv. Technol. 9 (1998) 527-535.

3. Dzhardimalieva G.I., Pomogailo A.D., Ponomare V.I., Atovmyan L.O., Shulga Yu.M., Starikov A.G.: *Synthesis and reactivity of metal-containing monomers.* 7. Synthesis and investigation of transition metal acrylates. Bull. Acad. Sci. USSR, Div. Chem. Sci. 37 (1988**)** 1352-1355 (Engl. Transl.).
4. Porollo N.P., Aliev Z.A., Dzhardimalieva G.I., IvlevaI.N., Uflyand I.E., Pomogailo A.D., Ovanesyan N.S.: *Synthesis and reactivity of metal-containing monomers.* 47. Synthesis and structure of salts of unsaturated dicarboxylic acids. Russ. Chem. Bull. 46 (1997) 362-370 (Engl. Transl.).
5. Nakamoto K.: *Infrared and Raman Spectra of Inorganic and Coordination Compounds.* Wiley and Sons, New York, USA., 1987.
6. Rozenberg A.S., Alexandrova E.I., Ivleva N.P., Dzhardimalieva G.I., Raevskii A.V., Kolesova O.I., Uflyand I.E., Pomogailo A.D.: *Reactivity of metal-containing monomers.* 48. Thermal transformations of cobalt(II) maleate. Russ. Chem. Bull. 47 (1998) 259–264 (Engl. Trans.).
7. Shuvaev A.T., Rozenberg A.S., Dzhardimalieva G.I., Ivleva N.P., Vlasenko V.G., Nedoseikina T.I., Lyubeznova T.A., Uflyand I.E., Pomogailo A.D.: *Synthesis and reactivity of metal-containing monomers. 50. Evolution of short-range surrounding of Fe atoms during thermal transformation of* $[Fe_3O(OOCCH=CHCOOH)^6]OH{\cdot}3H_2O$. Russ. Chem. Bull. 47 (1998**)** 1460–1465 (Engl. Trans.).
8. Granowski A., Wojtczak Z.: *The thermal decompositions of some transtion metal acrylates and polyacrylates.* J. Therm. Anal. 26 (1983) 233–239.
9. Wojtezak, Z.: J. Therm. Anal. 1990, 3*6*, 2357–2362.
10. Porai-Koshits M.A.: *In Kristallokhimiya, Itogi nauki i tekhniki* [Crystallochemistry, Advances in Science and Technology], VINITI, Moscow, 15 (1981) 13-45.